J. Membrane Biol. 104, 265–273 (1988)

The Journal of
Membrane Biology

A Flow EPR Study of Deformation and Orientation Characteristics of Erythrocyte Ghosts: Effects of Lysing and Resealing Conditions

Yasunori Fukushima* and Hideo Kon
Laboratory of Chemical Physics, National Institute of Diabetes and Digestive and Kidney Diseases, National Institutes of Health, Bethesda, Maryland 20892

Summary. The effects of various conditions in lysing and resealing the red cell membrane on the degree of ghost deformation and orientation in flow are investigated using the flow EPR and spin-label method. The relatively low deformability of the standard ghost, which is lysed and resealed, respectively, in hypotonic and isotonic NaCl-Tris buffer, is markedly enhanced by the presence of Mg-ATP, chlorpromazine, or Ca^{2+} ion during resealing. The effect is concentration dependent, and there is an optimal level for each treatment. Chlorpromazine and Ca^{2+} are also effective when added to the resealed ghosts. Mg^{2+} ion shows an opposite effect reducing the ghost deformability in flow at all concentrations. An isotonic lysis in NH_4HCO_3 solution with less osmotic stress substantially raises ghost deformability above that of the standard ghosts. These results are interpreted on the basis of a misalignment between the bilayer leaflets that is probably brought about during hypotonic lysis and its recovery to the nearly normal bilayer state by the agents used during or after resealing. The novel finding of deformability enhancing effect of calcium is assumed to be caused by the electrostatic expansion of the inner layer relative to the outer leaflet. The explanations are supported by the resealed ghost shapes observed before and after the treatments; shape recovery from the monoconcave spheroid toward biconcave discoid is observed in most cases concomitantly with improvements of flow characteristics.

Key Words EPR · spin label · erythrocyte ghost · deformability · bilayer compatibility

Introduction

Use of resealed red cell ghosts for studying rheological properties and morphological changes has the advantage of probing the underlying mechanism separately from the effects resulting from the change of cytoplasmic fluid viscosity. The whole cell deformability in flow, for example, is quite sensitive to the change in osmolality [19], while the isotonically resealed ghosts are rather insensitive over a range of osmolalities [8].

Previously, in the study of the flow-induced ghost deformation and orientation, we demonstrated that hypotonically resealed ghosts have a considerably reduced deformability from the isotonic controls, and that their behavior correlates well with the shift in the tetramer-dimer equilibrium of spectrin toward dimers [10].

In continuation of the study of resealed ghosts, we investigate in the present work the effects of lysing and resealing conditions on flow-induced ghost deformation and orientation. The effect of lysing and resealing conditions on the ghost volume, the amount of the residual hemoglobin, and the ghost extension recovery time have been studied by other workers [21–23]. The role of the membrane bilayer asymmetry as a determining factor of the red cell ghost morphology has been extensively demonstrated by Lange, Gough and Steck [14]. We will demonstrate further that perturbation of the intrinsic bilayer asymmetry by a lysing process has a profound effect on ghost deformability in flow, and that the perturbation can be reversed by various means including incubation with calcium at low concentrations during or after resealing.

To observe the ghost deformation and orientation, we use a flow EPR technique, in which spin-labeled ghosts are subjected to shear stress by flowing through a flat narrow channel and the accompanying EPR spectral change is monitored as a function of the flow rate. The spectral change occurs, not from a change in the microviscous environment of the spin-label molecules [7], but because of the flow-induced macroscopic deformation and orientation of ghosts and the attending change in spatial distribution of spin-label molecules. That such a flow-induced EPR spectral change serves as a useful parameter to assess the whole cell (ghost)

* *Present Address:* Department of Anesthesiology, Okayama University School of Medicine, 2-5-1 Shikata-cho, Okayama 700, Japan.

deformability was experimentally and theoretically demonstrated by the previous works [1–3, 12, 24–26].

Materials and Methods

Adenosine-5′-triphosphate (ATP), glutaraldehyde, chlorpromazine (CPZ), and sodium orthovanadate were purchased from Sigma Chemical Co.; dextran T500 (mean M.W. 500,000) was obtained from Pharmacia, and the spin label, 5-doxyl stearic acid, was purchased from Aldrich. All other reagents were of analytical grade.

Preparation of Spin-Labeled Resealed Ghost

Human venous blood from healthy donors was collected into heparinized (20 U/ml) tube and was used within 24 hr. The blood was centrifuged at 1500 × *g* for 5 min. After buffy coat and plasma were removed by aspiration, the remaining packed erythrocytes were washed three times with 5 mM Tris buffer containing 150 mM NaCl, 5 mM KCl (pH 7.4, 300 ± 5 mosmol/kg). About a 3-ml portion of packed erythrocytes, resuspended at 35% hematocrit, was spin labeled for 10 min at 37°C with 55.5 μg of 5-doxyl stearic acid coating inside a centrifuge tube, followed by washing twice with Tris-NaCl buffer. The labeled erythrocytes were resuspended at 50% hematocrit, kept in an ice bath for at least 30 min, lysed by adding 20 volumes of ice-cold lysing buffer (5 mM Tris, 7 mM NaCl, pH 7.4), and were kept at 0°C for 5 min. After centrifugation at 27,000 × *g* for 10 min to remove supernatant containing cell fragments and other debris, the lysed membrane was washed once with 20 volumes of cold lysing buffer. The pelleted membrane was incubated in 20 volumes of prewarmed (37°C) resealing buffer (5 mM Tris, 154 mM NaCl, 4 mM $MgSO_4$, pH 7.4) for 1 hr at 37°C, followed by 5 min cooling in an ice bath and centrifugation at 27,000 × *g* for 5 min to obtain "standard" resealed ghosts.

Effects of Presence of Some Reagents and Change of Preparative Conditions

Effects of deviating from the standard procedure described above, or presence of Mg-ATP, CPZ, Ca^{2+}, Mg^{2+} and some of their combinations at various stages of preparation on the flow deformation and orientation, and the morphology were examined. The detailed conditions are given in the Results section.

Ghost Deformability Measurement

Resealed spin-labeled ghosts (ca. 2 ml) were suspended in 5 mM Tris buffer containing 140 mM NaCl and 20% (wt/vol) dextran T500 to make up an isotonic suspension having 12% dextran concentration and ca. 2.8 × 10^9 cells/ml. The measurement of resealed ghost deformability was made by exploring the EPR spectral intensity change (Δh) occurring when the ghost suspension was driven through a flat quartz cell having 0.27 ± 0.01 mm wall-to-wall gap, 50 mm length, and 8 mm width. The flat surface was oriented perpendicularly to the magnetic field which was held fixed at H_{max} of 0.337 *T* (= 3370 gauss) where the maximal spectral change (Δh) occurred. H_{max} does not change with the flow rate or with the type of specimen, but varies with the type of spin label. Although H_{max} is located on a steep slope of the EPR absorption, the spectrometer stability is sufficient so that no detectable drift is observed during the measurement. Also, flowing a red cell suspension through the resonant cavity does not affect the quality factor of the cavity.

The normalized spectral change ($\Delta h/h$), where h is the maximum peak-to-trough height measured in the absence of flow, is plotted *vs.* volume flow rate to assess the degree of cell deformation and orientation in shear flow. The flow rate was linearly scanned while Δh values were stored on-line. In this experimental condition, the volume flow rate of 0.1 ml/sec corresponds to the wall shear rate of 1028.8/sec. All measurements were made at room temperature using Varian Model E-109 X-band EPR spectrometer with 100 kHz field modulation.

Morphological Examination

Ghost shapes were examined and photographs were taken using a Reichert light microscope equipped with a dark-field condenser and phase-contrast objective lenses. Some specimens were fixed in a glutaraldehyde solution (1%) at low temperatures for 1 to 2 hr, and others were examined immediately after preparation.

Results and Discussion

In the present flow EPR method, 5-doxyl stearate labels intercalated in the lipid phase of the membrane serve to report the degree of flow-induced cell deformation and orientation. A typical flow-induced spectral change in 5-doxyl stearate-labeled erythrocytes is illustrated in Fig. 1, and the definition of the normalized spectral changes ($\Delta h/h$) is indicated. When deformable cells (or ghosts) flow under shear stress, the two outer peaks in the EPR spectrum increase and the center peak decreases in intensity as the result of cell deformation with orientation approximately along the flow direction, which is arranged perpendicularly to the applied magnetic field. We use $\Delta h/h$ as a useful index for assessing the whole-cell deformability; the higher $\Delta h/h$ value indicates a greater cell deformation and orientation in flow. Cells which are not deformable tumble in flow, thereby averaging out $\Delta h/h$. Further details of the method are described in references [13] and [25].

Standard Ghost and Effect of Mg^{2+}

Freshly prepared resealed standard ghosts have a plump spheroid shape with apparent diameter of ca. 5 μm with slight crenation. The $\Delta h/h$ *vs.* flow rate curve (Fig. 2) rises gradually with flow rate but only up to $\Delta h/h$ = 0.2–0.3 even at the flow rate of 0.1 ml/sec, whereas normal erythrocytes should attain $\Delta h/h$ of 0.4–0.45 under the same conditions with a

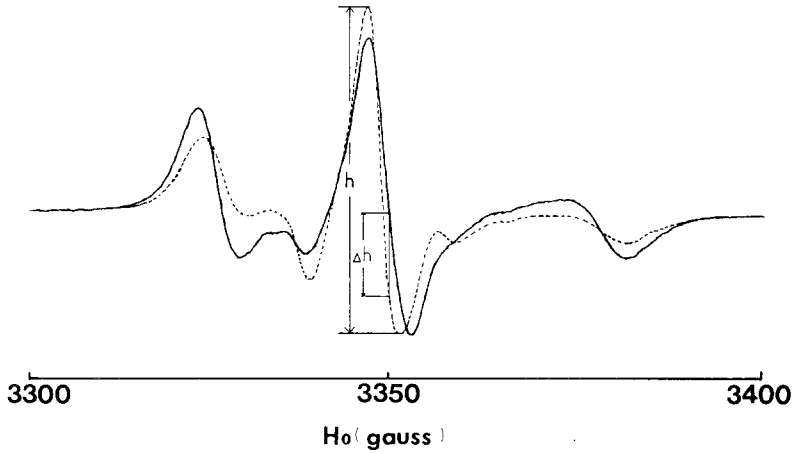

Fig. 1. A typical EPR spectrum of spin-labeled erythrocytes observed in the absence (. . .) and presence (—) of flow. Hematocrit 35%, extracellular dextran concentration 7.7%; h indicates the largest peak-to-trough height in the spectrum observed at rest, and Δh the maximal difference between the two spectra at 3370 gauss

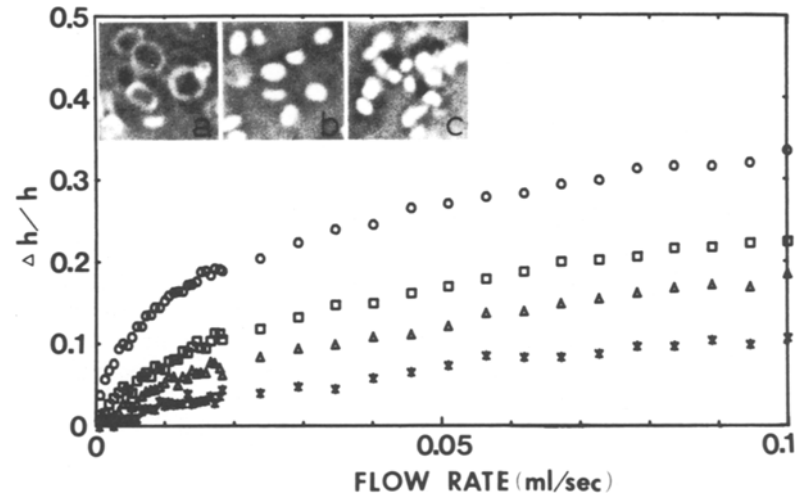

Fig. 2. Effects of Mg^{2+} on $\Delta h/h$ *vs.* flow rate curve and ghost shape. Spin-labeled red blood cells were lysed in 20 vol of ice-cold buffer (5 mM Tris, 7 mM NaCl, pH 7.4); pelleted membrane was incubated at 37°C for 1 hr in a prewarmed resealing buffer (5 mM Tris, 154 mM NaCl, pH 7.4) containing $MgSO_4$ (mM): 0 (○), 4 (□), 10 (△), 30 (*). *Inset:* Crenation was enhanced with $MgSO_4$ concentration (mM): (*a*) 0, (*b*) 4, (*c*) 30

sharp rise at the start of flow. Thus the flow-induced deformation of the standard ghost is shown relatively low. If $MgSO_4$ is absent from the resealing solution, the overall $\Delta h/h$ is enhanced considerably, while an increase in $MgSO_4$ concentration has a suppressive effect on $\Delta h/h$ (Fig. 2), and at the same time crenation in ghost shape becomes more evident. The crenated standard ghost shape is explained by Lange et al. [14] to be the result of the relatively expanded outer leaflet caused by phospholipid migration in hemolysis with the process being intensified by cationic charges bound to the cytoplasmic side in the isotonic resealing solution. Mg^{2+} ions are apparently more potent than Na^+ or K^+ with respect to the effect on shape as well as on $\Delta h/h$.

Along the same line of reasoning, and on the basis of the bilayer coupling hypothesis [29], we propose that the resulting misalignment between the two leaflets of the membrane affects the flow-induced deformation and orientation characteristics of ghosts. As shown in the following, such an effect goes beyond that which has been attributed to the "shape factor" that has been considered to manifest itself only in the low-to-medium shear rate region of the viscoelastic properties [16–18]. The initial stage of echinocytosis or stomatocytosis is the typical case of the latter [9, 19]. We present several pieces of evidence to support the above hypothesis.

Effect of Mg-ATP

The presence of ATP (<1 mg/ml) and Mg^{2+} at the time of resealing is found to cause a remarkable enhancement of $\Delta h/h$ values in the standard ghost over the entire range of the flow rate (0–0.1 ml/sec) (Fig. 3). The effect peaks at ca. 0.5–1 mg ATP/ml, above which the $\Delta h/h$ starts decreasing. The monoconcave spheroid shape of the standard ghost is transformed to the biconcave discoid with increasing concentration of ATP, and eventually some sto-

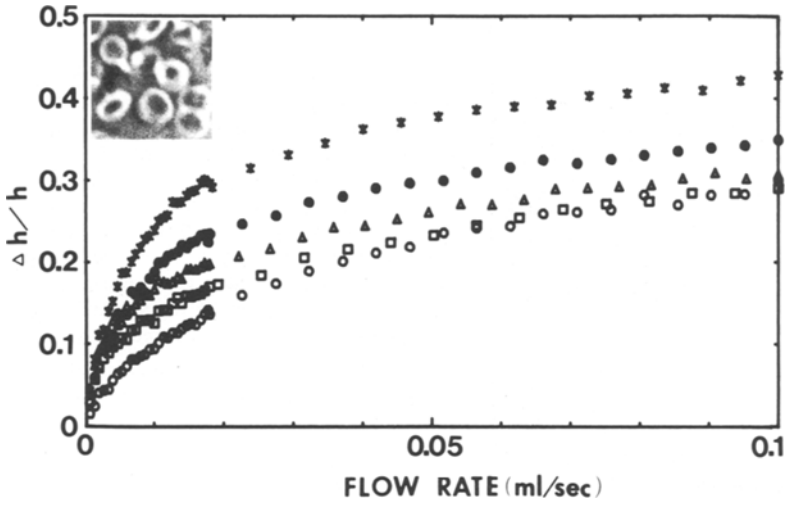

Fig. 3. Effects of Mg-ATP on $\Delta h/h$ *vs.* flow rate curve and ghost shape. Spin-labeled red blood cells were lysed in 20 vol of ice-cold buffer (5 mM Tris, 7 mM NaCl, pH 7.4); pelleted membrane was incubated at 37°C for 1 hr in a prewarmed resealing buffer (5 mM Tris, 154 mM NaCl, 4 mM $MgSO_4$, pH 7.4) containing ATP (mg/ml): 0 (○), 0.1 (□), 0.2 (△), 0.5 (*), 1 (●). *Inset:* The cell shape is mostly biconcave discoid at ATP concentration of 0.5 mg/ml

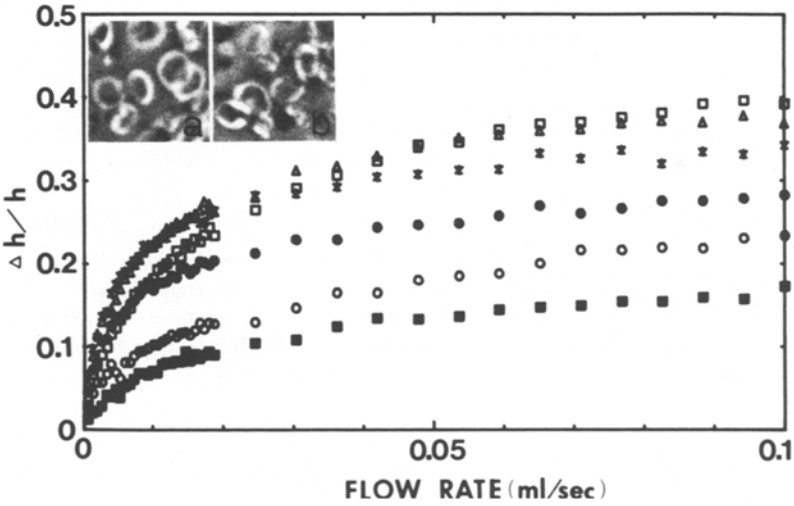

Fig. 4. Effects of CPZ on $\Delta h/h$ *vs.* flow rate curve and ghost shape. Spin-labeled red blood cells were lysed in 20 vol of ice-cold buffer (5 mM Tris, 7 mM NaCl, pH 7.4); pelleted membrane was incubated at 37°C for 1 hr in a prewarmed resealing buffer (5 mM Tris, 154 mM NaCl, 4 mM $MgSO_4$, pH 7.4) containing CPZ (μM): 0 (○), 50 (□), 100 (△), 200 (*), 300 (●), 400 (■). *Inset:* (*a*) biconcave discoid at 100 μM CPZ, (*b*) 400 μM CPZ; stomatocytic shape was discernible above 200 μM

matocytic shapes begin to show above 0.5 mg ATP/ml. Orthovanadate, a potent ATPase inhibitor, added at 0.5–2 μM at the start of resealing incubation completely quenches the enhancing effect of ATP with no apparent concentration dependence. The experiments in which orthovanadate is added at various time intervals after incubation has started demonstrate that the $\Delta h/h$ enhancing effect by ATP is practically completed in ca. 30 min.

Previously, Seigneuret and Devaux [27] showed, in echinocytes formed by ATP depletion and in ghost preparations, that the presence of Mg-ATP causes accelerated transverse diffusion of phosphatidylserine and phosphatidylethanolamine from the outer to the inner layer of the membrane, thereby restoring the biconcave discoid shape suggesting recovery of a nearly native state of asymmetric phospholipid distribution as well. The present results further demonstrate that such transverse shift of phospholipid population is likely to be the reason for the enhancement by Mg-ATP of deformation and orientation of ghosts in flow. The observation that the ATP-induced enhancement of $\Delta h/h$ extends over the whole range of the flow rate indicates that the effect is not attributable simply to the type of shape recovery in which the change in $\Delta h/h$ is limited to the low-to-middle flow rate region [16–18].

Effect of CPZ

If the increase in $\Delta h/h$ values and restoration of the shape by ATP are the results of transbilayer phospholipid diffusion to restore a near normal state of bilayer asymmetry, an essentially similar effect may possibly be achieved by applying an amphiphilic agent, chlorpromazine, which preferentially populates and expands the cytoplasmic side of the bilayer [5, 6, 20].

As shown in Fig. 4, the observed $\Delta h/h$ of ghosts resealed in the presence of CPZ shows a marked enhancement with the maximum effect occurring

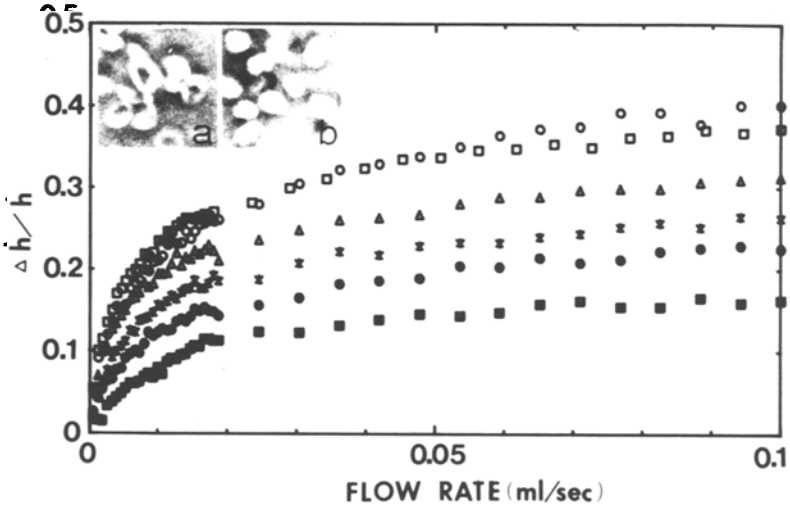

Fig. 5. Effects of CPZ on $\Delta h/h$ *vs.* flow rate curve and shape of ATP-resealed ghosts. Spin-labeled red blood cells were lysed in 20 vol of ice-cold buffer (5 mM Tris, 7 mM NaCl, pH 7.4); pelleted membrane was incubated at 37°C for 1 hr in a prewarmed resealing buffer (5 mM Tris, 154 mM NaCl, pH 7.4) containing 0.5 mg/ml ATP. Resealed ghosts were further incubated in the same buffer containing CPZ (μM); 0 (○), 50 (□), 100 (△), 200 (*), 300 (●), 400 (■) at 37°C for 1 hr. *Inset:* (*a*) stomatocytic at 100 μM, (*b*) stomatocytic at 400 μM; stomatocyte formation is intensified here compared with that in Fig. 4

between 50 and 100 μM CPZ. The ghost morphology changes from that of the standard ghost via the biconcave discoid at 50–100 μM CPZ to the stomatocytic above 200 μM CPZ. Stomatocyte formation in normal erythrocyte is clearly discernible in 100–200 μM CPZ, but somewhat higher concentrations are required in the standard ghosts. This is consistent with the assumed lipid-deficient state of the inner layer to start with.

The same results were obtained by adding CPZ after resealing in Tris-NaCl solution and incubating for 1 hr at 37°C. The $\Delta h/h$ enhancement covers the whole region of the flow rate, again suggesting that the effect is not due to the shape factor alone. The incubation temperature (37°C or ambient) has little effect on the final result. The enhancement of $\Delta h/h$ with CPZ, even at a near optimal concentration, is usually less than that obtained by incubating with the optimal amount of ATP. This may be due to the fact that the "restored" membrane asymmetry of the bilayer incorporated with CPZ still represents a deviation from the normal bilayer coupling state of the intact membrane to the extent that both layers are augmented by the presence of CPZ preferentially in the inner leaflet. If ghosts are first resealed with ATP (0.5 mg/ml), a further treatment with CPZ (100–200 μM) partially reverses the effect of the former, reducing $\Delta h/h$ values, and at the same time, a greater population of stomatocyte is detected compared with the system treated with CPZ alone at the same concentration (Fig. 5). This observation indicates that essentially the same mechanism, i.e. a relative expansion of the inner layer, could be the end result of the use of both ATP and CPZ.

Effect of Lysing in Isotonic NH_4HCO_3

In their study on the relationship between ghost crenatability and the type of lysing media, Lange et al. [14] showed that hemolysis in 150 mM NH_4HCO_3 yields ghosts having a suppressed crenatability when exposed to a crenating reagent or an isotonic medium. The decrease of crenatability was attributed to a reduced osmotic stress attending hemolysis, thus preventing shift of phospholipids from the inner to the outer leaflet on lysing as is assumed to occur in an ordinary hypotonic lysing.

To test if the same procedure may also influence $\Delta h/h$, we have lysed red cells in 5 mM Tris buffer (pH 7.4) containing 150 mM NH_4HCO_3 at 0°C for various lengths of time followed by resealing at 37°C in the same medium. The resulting resealed ghosts, having mostly discoid shape mixed with a small population of stomatocytes (Fig. 6), are bulkier and appear to contain more residual hemoglobin than the control which is lysed and resealed in NaCl. As shown in Fig. 6, the ghosts have much higher $\Delta h/h$ than the control over the whole range of the flow rate. Changing lysis duration (5–20 min) has no effect, indicating that lysis, though gentle, is complete in less than 5 min.

The result is consistent with the idea that at the time of or following lysis in hypotonic NaCl solution, there is a shift in the lipid composition in favor of the outer leaflet, and that lysing under a mild condition, such as with NH_4HCO_3, helps preserve the intact bilayer asymmetry.

When the ghosts lysed in NH_4HCO_3 are resealed in a NaCl-NH_4HCO_3 mixed solution, the overall $\Delta h/h$ values become lower as the fraction of NaCl increases than those for the ghosts treated with NH_4HCO_3 throughout, particularly in the low flow rate range. Conversely, when ghosts lysed in 7 mM NaCl solution are resealed in the mixed resealing solution, the $\Delta h/h$ values are somewhat enhanced especially in the low flow rate range as the fraction of NH_4HCO_3 is increased, but never become as high as in ghosts lysed and resealed in NH_4HCO_3 only. As the NaCl fraction is increased, the morphology changes concomitantly toward that

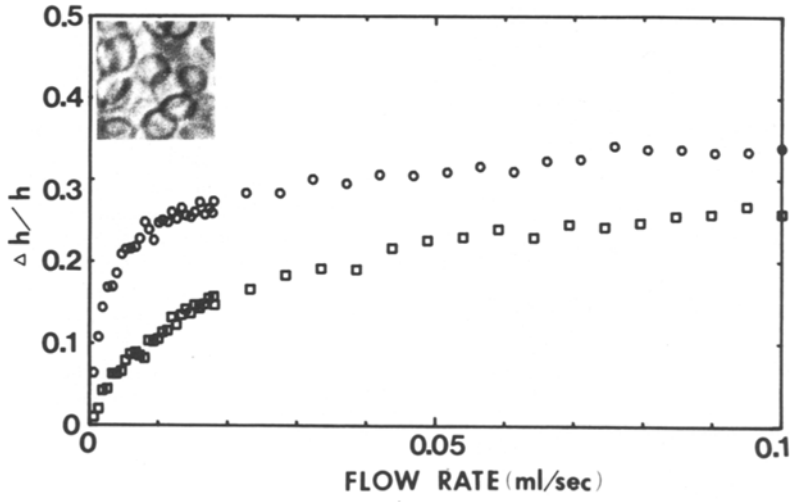

Fig. 6. Effects of lysing in isotonic NH_4HCO_3 on $\Delta h/h$ *vs.* flow rate curve and ghost shape. Spin-labeled red blood cells were lysed in 20 vol of ice-cold 5 mM Tris buffer (pH 7.4) containing 150 mM NH_4HCO_3. Pelleted membrane was incubated in the same buffer at 37°C for 1 hr. (○) lysed and resealed in NH_4HCO_3, (□) standard resealed ghost. *Inset:* Cell shapes are biconcave discoid

of the standard ghost. This action of different cations in resealing, which increases up to a NaCl/NH_4HCO_3 ratio of about 1 : 1, can be understood on the basis of cations effecting a relative contraction of the more negatively charged cytoplasmic side of the membrane by charge neutralization in which Na^+ ions are more effective than NH_4^+.

If the ghosts lysed in NH_4HCO_3 are resealed in a medium in the presence of 0.5 mg/ml ATP with 4 mM Mg^{2+}, the $\Delta h/h$ values decrease by ca. 30%; this may be due to over-compensation of the bilayer asymmetry by the lipid transport mediated by Mg-ATP.

Effect of Ca^{2+} Ions

Echinocyte formation in erythrocytes induced by Ca^{2+} loading with the ionophore A23187 with concomitant loss of the whole-cell deformability in flow has been extensively studied [4, 26]. Similar findings have been reported for ghosts prepared from cells loaded with various Ca^{2+} concentrations of the order of 1 mM or higher, and the loss of deformability was explained by transglutaminase-mediated protein cross-linking [8]. However, the direct effect of Ca^{2+} ions affecting the membrane deformability at lower concentrations has not been completely clarified. We have re-examined the effect of Ca^{2+} at low concentrations (<2 mM) using standard ghost preparations. When resealing is carried out at 37°C in the standard resealing medium containing various concentrations of Ca^{2+}, the $\Delta h/h$ values become substantially elevated over the whole range of the flow rate (Fig. 7), indicating an increased flow-induced deformation and orientation. The effect is Ca^{2+} concentration dependent, and is detectable even at an added Ca^{2+} concentration of as low as 20 μM. (The background concentration of Ca^{2+} in the final solution, measured with a Ca^{2+} electrode and calibrated with standard calcium solutions, is 30 ± 10 μM in our preparations.) At the same time, the shape of the ghosts changes from the spheroid echinocytic of the standard ghosts to bioconcave discoid (Fig. 7). The $\Delta h/h$ values continue to increase with the Ca^{2+} concentration and peak in the range 0.5–2 mM depending upon the blood source and/or the preparation, and decrease as the Ca^{2+} concentration is increased further. The effect is virtually complete at 30-min incubation. An identical result was obtained by adding Ca^{2+} to the ghosts resealed in advance in isotonic Tris-NaCl, and incubating at 37°C for 1 hr. In this case also, the Ca^{2+} effect is complete in ca. 30 min. Incubating the Ca^{2+}-treated ghosts with EGTA (2 mM) for 15 min at 37°C partially (<50%) reverses the Ca^{2+}-induced $\Delta h/h$ enhancement, and the shape reverts to that of the standard ghost with some vesiculation occurring. Washing the Ca^{2+}-treated resealed ghosts with Tris-NaCl buffer does not affect the Ca^{2+} effect.

Treating ghosts with CPZ (~100 μM) following resealing at a concentration (e.g., 0.5 mM) of Ca^{2+} usually enhances $\Delta h/h$ values further before they start to decrease at a higher CPZ concentration (Fig. 8). If the Ca^{2+} concentration is adjusted to maximize the Ca^{2+} effect for a particular preparation, then the increment of $\Delta h/h$ by the same level of CPZ is smaller or $\Delta h/h$ values show decreases.

When ghosts lysed in Tris-NH_4HCO_3 are resealed in NH_4HCO_3 in the presence of Ca^{2+} ion (1 mM), the $\Delta h/h$ values are reduced by <30% from that of the control without Ca^{2+}. However, if Ca^{2+} is added after completion of resealing in NH_4HCO_3 solution, then the suppressing effect is much smaller, probably because of the time required for Ca^{2+} to diffuse into the ghost which is prepared in NH_4HCO_3 buffer.

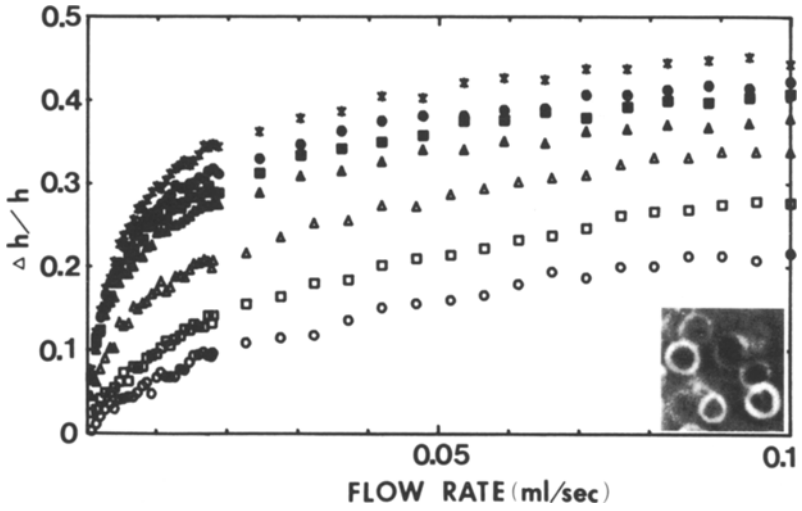

Fig. 7. Effects of Ca^{2+} ion on $\Delta h/h$ *vs.* flow rate curve and ghost shape. Spin-labeled red blood cells were lysed in 20 vol of ice-cold buffer (5 mM Tris, 7 mM NaCl, pH 7.4); pelleted membrane was incubated at 37°C for 1 hr in a prewarmed resealing buffer (5 mM Tris, 154 mM NaCl, 4 mM $MgSO_4$, pH 7.4) containing $CaCl_2$ (mM): 0 (○), 0.04 (□), 0.1 (△), 0.5 (*), 1 (●), 1.5 (■), 2 (▲). *Inset:* Cell shape is biconcave discoid at Ca^{2+} concentration of 0.5 mM

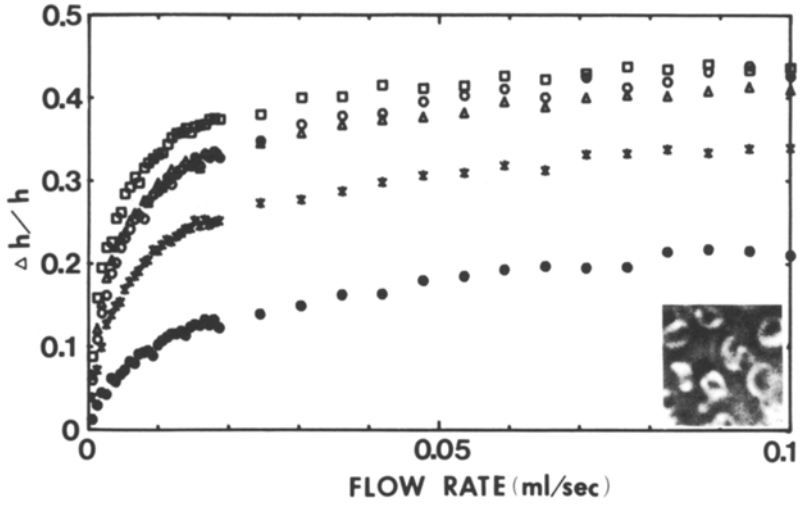

Fig. 8. Effects of CPZ on $\Delta h/h$ *vs.* flow rate curve and shape of Ca^{2+}-resealed ghosts. Spin-labeled red blood cells were lysed in 20 vol of ice-cold buffer (5 mM Tris, 7 mM NaCl, pH 7.4); pelleted membrane was incubated at 37°C for 1 hr in a prewarmed resealing buffer (5 mM Tris, 154 mM NaCl, 4 mM $MgSO_4$, pH 7.4) containing 0.5 mM $CaCl_2$. Resealed ghosts were further incubated in the same buffer containing CPZ (μM); 0 (○), 100 (□), 200 (△), 300 (*), 400 (●). *Inset:* CPZ at 200 μM causes stomatocyte formation

Such an unambiguous effect of Ca^{2+} ion to improve the flow-induced ghost deformation and orientation in the standard preparation has never been reported before. It is an effect opposite to what one normally expects in Ca^{2+}-erythrocyte membrane interactions. For example, Ca^{2+} ion has been shown to be a potent crenating agent of ghost when applied in the absence of other electrolytes [28]. In erythrocytes, Ca^{2+}-loading causes a loss of the whole-cell deformability as the result of K^+ and water extrusion [4, 26]. The present results, which are at variance with other observations [8], clearly demonstrate a different type of direct action of Ca^{2+} at low concentrations on the ghost membrane. Judging from the simultaneously observed discoid shape recovery, such a Ca^{2+} action should involve bringing the state of bilayer coupling closer to the native condition, either by shifting phospholipid population between the leaflets, or through an electrostatic contraction or expansion of one against the other. When the Ca^{2+} concentration is not optimal, an addition of CPZ can make a further improvement. Similarly, if the bilayer asymmetry is maintained nearly intact as in the case of a gentle lysis in NH_4HCO_3 solution, a further action by Ca^{2+} would cause an imbalance and contribute to a decrease in $\Delta h/h$. Since washing the ghosts resealed in the presence of Ca^{2+} with buffer solution or adding Ca^{2+} after resealing in NH_4HCO_3 has only a minor effect on $\Delta h/h$ and morphology, the sites of Ca^{2+} action are more likely to be on the cytoplasmic side of the membrane. Also, the fact that an effective Ca^{2+} concentration of as low as 50 μM exerts a sizable effect, that EGTA applied after resealing with Ca^{2+} does not completely reverse the Ca^{2+} effect, and the inability of Mg^{2+} to induce a similar effect suggest that the action may involve, at least in part, some Ca^{2+}-specific interaction sites on the cytoplasmic

surface of the bilayer and/or the cytoskeletal protein structure.

The precise mechanism of the Ca^{2+} effect is still a matter of speculation, but we are inclined to explain it as based upon the relative expansion of the inner layer; namely, before Ca^{2+} ion is introduced, we believe the negative charges on the inner surface are neutralized by Na^{+} ions with a resultant surface contraction to which the spheroid monoconcave shape of the standard ghost is attributable [14]. With Ca^{2+} ions replacing some of the Na^{+} ions and introducing their extra positive charges, Ca^{2+} ions can expand the inner layer to compensate for the surplus outer layer surface brought about during lysis. Such a model was postulated to explain the observed changes in the radius of curvature in human erythrocyte membrane vesicles due to inorganic cations [15]; however, in that model system, Ca^{2+} and Mg^{2+} exerted similar effects in contrast to the present results.

Concluding Remarks

The data presented here can be most consistently interpreted by assuming that whenever the natural asymmetry existing between the two leaflets in ghosts is perturbed by lysing, the effect is manifested not only in morphological changes but also as a reduced flow-induced deformation and orientation, and the process can be reversed by means of phospholipid transfer in the opposite direction, augmenting the phospholipid deficient side with some reagent, or expanding it by introducing extra charges on the same side.

The morphological change is one of the several known factors which affect the whole cell (or ghost) deformability in flow [19]; however, its consequence expressed in the suspension viscosity [16, 17] or whole cell deformability [18, 24] measurements has been thought to manifest itself under low-to-medium shear rates and to diminish rapidly as the shear rate approaches 1000/sec. When the morphological change advances to the stage of spherocyte formation, the attending change in rheological properties that extends to a higher shear region has been understood as due to another factor such as reduced surface area-to-volume ratio. While such may be the case, especially when some membrane material loss can be observed, the mechanism underlying morphological changes, namely the type of misalignment between the bilayers described above, can cause more extensive effects than what has been previously shown, and the effects are manifested in the high shear rates as well. Such a misalignment is likely to alter the bending modulus of the membrane system as a whole including the spectrin network, and would affect the tank-treading motion that is required for maintaining a steady orientation in flow [11]. To the extent that the orientation is unstable, $\Delta h/h$ values should be decreased by motional averaging.

The authors thank Dr. Makio Murayama for his help in photomicrography.

References

1. Bitbol, M., Leterrier, F. 1982. Measurement of the erythrocyte orientation in a flow by spin labeling. I. Comparison between experimental and numerically simulated E.P.R. spectra. *Biorheology* **19:**669–680
2. Bitbol, M., Leterrier, F., Quemada, D. 1985. Measurement of the erythrocyte orientation in a flow by spin labeling. III. Erythrocyte orientation and rheological conditions. *Biorheology* **22:**43–53
3. Bitbol, M., Quemada, D. 1985. Measurement of the erythrocyte orientation in a flow by spin labeling. II. Phenomenological models for erythrocyte orientation rate. *Biorheology* **22:**31–41
4. Clark, M.R., Mohandas, N., Feo, C., Jacobs, M.S., Shohet, S.B. 1981. Separate mechanisms of deformability loss in ATP-depleted and Ca-loaded erythrocytes. *J. Clin. Invest.* **67:**531–539
5. Deuticke, B. 1968. Transformation and restoration of biconcave shape of human erythrocytes induced by amphiphilic agents and changes of ionic environment. *Biochim. Biophys. Acta* **163:**494–500
6. Fujii, T., Sato, T., Tamura, M., Wakatsuki, M., Kanaho, Y. 1979. Shape changes of human erythrocytes induced by various amphipathic drugs acting on the membrane of intact cells. *Biochem. Pharmacol.* **28:**613–620
7. Griffith, O.H., Jost, P.C. 1976. Lipid spin labels in biological membranes. *In:* Spin Labeling, Theory and Applications. L.J. Berliner, editor. pp. 453–523. Academic, New York
8. Heath, B.P., Mohandas, N., Wyatt, J.L., Shohet, S.B. 1982. Deformability of isolated red blood cell membranes. *Biochim. Biophys. Acta* **691:**211–219
9. Ito, T., Kon, H. 1987. The copper-induced deformability loss and echinocyte formation in human erythrocyte: An electron paramagnetic resonance study. *Toxicol. Appl. Pharmacol.* **88:**242–254
10. Ito, T., Kon, H. 1988. A flow EPR study of deformation and orientation characteristics of erythrocyte ghosts: A possible effect of an altered state of cytoskeletal network. *J. Membrane Biol.* **101:**57–65
11. Keller, S.R., Skalak, R. 1982. Motion of a tank-treading ellipsoidal particle in a shear flow. *J. Fluid Mech.* **120A:**27–47
12. Kon, K., Noji, S., Kon, H. 1983. Spin label study of erythrocyte deformability. III. Further characterization of electron spin resonance spectral change in shear flow. *Blood Cells* **9:**427–438
13. Kon, K., O'Bryan, E.R., Kon, H. 1985. Effect of the presence of hardened erythrocytes on deformation-orientation characteristics of normal erythrocytes in shear flow studied by the spin label method. *Biorheology* **22:**105–117

14. Lange, Y., Gough, A., Steck, T.L. 1982. Role of the bilayer in the shape of the isolated erythrocyte membrane. *J. Membrane Biol.* **69:**113–123
15. Lin, G.S.B., Macey, R.I. 1978. Shape and stability changes in human erythrocyte membranes induced by metal ions. *Biochim. Biophys. Acta* **512:**270–283
16. Meiselman, H.J. 1977. Flow behavior of ATP-depleted human erythrocytes. *Biorheology* **14:**111–126
17. Meiselman, H.J. 1978. Rheology of shape transformed human red cells. *Biorheology* **15:**225–237
18. Meiselman, H.J. 1981. Morphological determinants of red cell deformability. *Scand. Clin. Lab. Invest.* **156:**27–34
19. Mohandas, N., Clark, M.R., Jacobs, M.S., Shohet, S.B. 1980. Analysis of factors regulating erythrocyte deformability. *J. Clin. Invest.* **66:**563–573
20. Mohandas, N., Feo, C. 1975. A quantitative study of the red cell shape changes produced by anionic and cationic derivatives of phenothiazine. *Blood Cells* **1:**373–384
21. Nash, G.B., Meiselman, H.J. 1983. Red cell and ghost viscoelasticity: Effects of hemoglobin concentration and in vivo aging. *Biophys. J.* **43:**63–73
22. Nash, G.B., Meiselman, H.J. 1985. Effects of preparative procedures on the volume and content of resealed red cell ghosts. *Biochim. Biophys. Acta* **815:**477–485
23. Nash, G.B., Tran-Son-Tay, R., Meiselman, H.J. 1986. Influence of preparative procedures on the membrane viscoelasticity of human red cell ghosts. *Biochim. Biophys. Acta* **855:**105–114
24. Noji, S., Inoue, F., Kon, H. 1981. Spin label study of erythrocyte deformability. I. Electron spin resonance spectral change under shear flow. *Blood Cells* **7:**410–411
25. Noji, S., Kon, H., Taniguchi, S. 1984. Spin label study of erythrocyte deformability. IV. Relation of ESR spectral change with deformation and orientation of erythrocytes in shear flow. *Biophys. J.* **46:**349–355
26. Noji, S., Taniguchi, S., Kon, H. 1987. Spin label study of erythrocyte deformability. Ca^{2+}-induced loss of deformability and the effects of stomatocytogenic reagents on the deformability loss in human erythrocytes in shear flow. *Biophys. J.* **52:**221–227
27. Seigneuret, M., Devaux, P.D. 1984. ATP-dependent asymmetric distribution of spin-labeled phospholipids in the erythrocyte membrane: Relation to shape changes. *Proc. Natl. Acad. Sci. USA* **81:**3751–3755
28. Sheetz, M.P. 1977. Cation effects on cell shape. *In:* Cell Shape and Surface Architecture. J.P. Revel, U. Henning and C.F. Fox, editors. pp. 559–567. Alan R. Liss, New York
29. Sheetz, M.P., Singer, S.J. 1974. Biological membrane as bilayer couples. A molecular mechanism of drug-erythrocyte interactions. *Proc. Natl. Acad. Sci. USA* **71:**4457–4461

Received 21 March 1988; revised 13 May 1988